Two synaptojanin 1 isoforms are recruited to clathrin-coated pits at different stages

Rushika M. Perera*, Roberto Zoncu*†, Louise Lucast*†, Pietro De Camilli*†‡, and Derek Toomre*‡

*Department of Cell Biology and †Howard Hughes Medical Institute, Kavli Institute for Neuroscience and Program in Cellular Neuroscience, Neurodegeneration and Repair, Yale University School of Medicine, New Haven, CT 06510

Contributed by Pietro De Camilli, November 3, 2006 (sent for review October 23, 2006)

Phosphoinositides are thought to play an important role in clathrin-coated pit (CCP) dynamics. Biochemical and structural studies have shown a direct interaction of phosphatidylinositol (4,5)-bisphosphate [PI(4,5)P_2] with endocytic clathrin adaptors, whereas functional studies using cell-free systems or intact cells have demonstrated the importance of PI(4,5)P_2 synthesis and dephosphorylation in clathrin coating and uncoating, respectively. Furthermore, genetic manipulations of kinases and phosphatases involved in PI(4,5)P_2 metabolism result in major defects in synaptic vesicle recycling and other forms of clathrin-dependent endocytosis. However, live imaging studies of these enzymes at CCPs have not been conducted. We have used multicolor total internal reflection fluorescence microscopy (TIRFM) to visualize the spatial-temporal recruitment of synaptojanin 1 (SJ1), a polyphosphoinositide phosphatase, and its binding partner endophilin to CCPs. Strikingly, we observed differential temporal recruitment of the two major SJ1 splice variants to CCPs. The 145-kDa isoform, the predominant isoform expressed in the brain, was rapidly recruited as a "burst," together with endophilin, at a late stage of CCP formation. In contrast, the nonneuronal ubiquitously expressed 170-kDa isoform of SJ1 was present at all stages of CCP formation. These results raise the possibility that dynamic phosphoinositide metabolism may occur throughout the lifetime of a CCP.

dynamin | endocytosis | endophilin | phosphoinositides | phosphatidylinositol (4,5)-bisphosphate

Strong evidence indicates that phosphoinositides, in particular phosphatidylinositol (4,5)-bisphosphate [PI(4,5)P_2], play a critical role in endocytosis by their property to function as coreceptors for endocytic factors (1–5). For example, PI(4,5)P_2 is a ligand for all known clathrin adaptors and many of their accessory factors, as well as for dynamin, a GTPase implicated in the fission of endocytic vesicles from the plasma membrane (5, 6). The physiological role of PI(4,5)P_2 in endocytosis was strongly supported by the identification and characterization of a polyphosphoinositide phosphatase, synaptojanin 1 (SJ1), as a clathrin-coat accessory factor (2, 3). SJ1 contains two inositol phosphatase domains arranged in tandem (see Fig. 1*A*). The N-terminal SacI domain dephosphorylates predominantly PI(3)P and PI(4)P, whereas the centrally located 5-phosphatase domain dephosphorylates PI(4,5)P_2 and PI(3,4,5)P_3 at the 5′ position of the inositol ring (2, 3, 7, 8). The C-terminal region acts primarily as a protein–protein interaction domain and was implicated in its subcellular targeting (2, 9–12). This region is alternatively spliced giving rise to 145- and 170-kDa SJ1 isoforms, referred to henceforth as SJ1-145 and SJ1-170, respectively (2, 13). The SJ1-170 splice variant, whose function is currently unknown, bears an additional C-terminal tail that contains binding sites for clathrin, the clathrin adaptor AP2, and the accessory factor Eps15 (Fig. 1*A*) (9, 12). Although both isoforms are ubiquitously expressed, SJ1-145 is present at very high concentrations in presynaptic nerve terminals of the adult brain (2, 13).

The portion of the C-terminal region common to both SJ1-145 and SJ1-170 interacts with the SH3 domains of a variety of proteins implicated in endocytosis and signaling: endophilin, amphiphysin, syndapin/pacsin, intersectin, and many others (10, 14–18). Endophilin is thought to be a particularly important interactor of SJ1 and to play a major role in its recruitment to sites of endocytosis (2, 15, 19, 20). In both flies and worms, mutations of endophilin and synaptojanin have similar phenotypes, and loss of endophilin results in destabilization and mislocalization of synaptojanin (21–24). Endophilin, which binds synaptojanin by its C-terminal SH3 domain, also contains an N-terminal BAR domain. The latter has curvature-generating and -sensing properties and may participate in the generation and maturation of endocytic bud necks (25–27). Mammalian cells express three isoforms of endophilin, with endophilin 2 (Endo2) being the predominant isoform in nonneuronal cells (15).

Most SH3 domain-containing proteins that bind SJ1, including endophilin, also interact with dynamin (15, 17, 18). This biochemical link to dynamin, together with the accumulation of coated vesicles at synapses of SJ1 knockout mice, has led to the hypothesis that the main function of SJ1-mediated hydrolysis of PI(4,5)P_2 is to facilitate clathrin uncoating after fission (3, 5, 28).

Despite the large body of biochemical and genetic studies on synaptojanin and endophilin, which underscore their central role in endocytosis, the precise timing of their recruitment to endocytic sites in relation to other endocytic proteins is unknown. Moreover, the relatively lower-level expression of these proteins in nonneuronal cells has made their localization outside the brain, where they are present at high concentration, difficult to assess. Functional differences between SJ1-145 and SJ1-170 isoforms have also not been investigated.

In this study, we have capitalized on the thin optical sectioning and sensitivity of total internal reflection fluorescent microscopy (TIRFM) to monitor the dynamics of fluorescently tagged endophilin and SJ1 in relation to the formation and disappearance of clathrin-coated pits (CCPs). We show that endophilin mediates the recruitment of SJ1-145, and that these proteins appear as a transient burst during late stages of CCP formation. We also show that, unexpectedly, SJ1-170 is present throughout the formation and maturation of CCPs.

Results

Endophilin Is Recruited to CCPs at a Late Stage. Because endophilin is a major binding partner of synaptojanin (Fig. 1*A*), we first investigated its spatial-temporal dynamics in live cells and in

Author contributions: R.M.P., R.Z., P.D.C., and D.T. designed research; R.M.P. performed research; L.L., P.D.C., and D.T. contributed new reagents/analytic tools; R.M.P. and R.Z. analyzed data; and R.M.P., P.D.C., and D.T. wrote the paper.

Abbreviations: CCP, clathrin-coated pits; LCa, clathrin light chain; SJ1, synaptojanin 1; Endo1/2, endophilin 1/2; mRFP, monomeric red fluorescent protein; TIRFM, total internal reflection fluorescence microscopy; SJ1-145, 145-kDa SJ1 isoform; SJ1-170, 170-kDa SJ1 isoform; Dyn2, dynamin 2; PI(4,5)P_2, phosphatidylinositol (4,5)-bisphosphate.

Freely available online through the PNAS open access option.

‡To whom correspondence may be addressed. E-mail: derek.toomre@yale.edu or pietro.decamilli@yale.edu.

This article contains supporting information online at www.pnas.org/cgi/content/full/0609795104/DC1.

© 2006 by The National Academy of Sciences of the USA

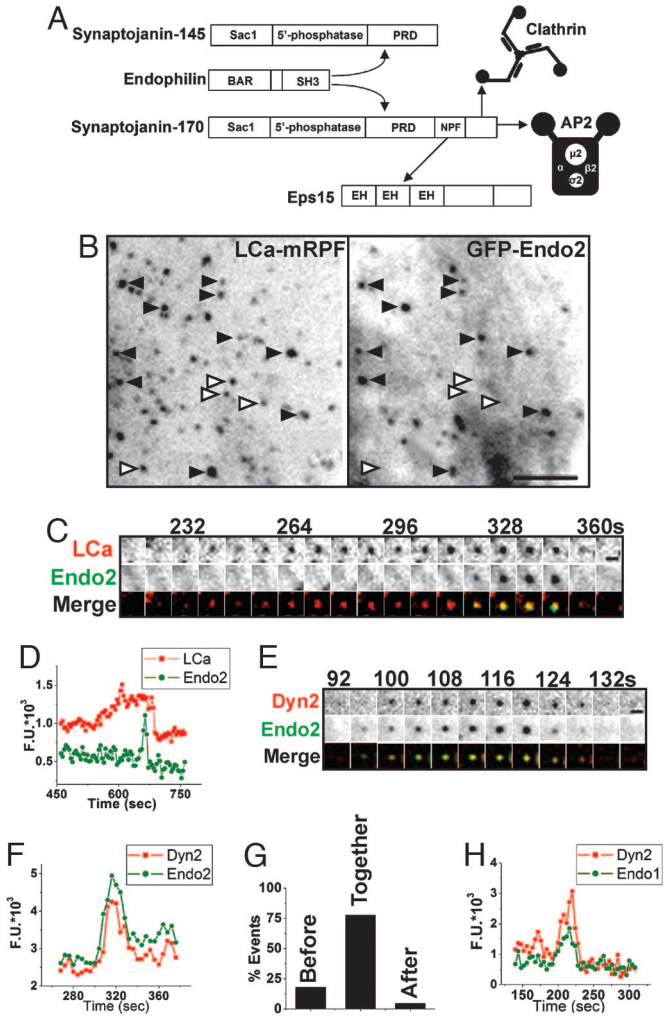

Fig. 1. Accumulation of endophilin with dynamin at late stage CCPs. (*A*) Major splice variants of SJ1: SJ1-145 (highly enriched in brain) and SJ1-170 (ubiquitously expressed). Endophilin interacts with the proline-rich domain (PRD) of SJ1, which is common to both isoforms, by its SH3 domain. The C-terminal region specific to SJ1-170 contains binding sites for the ear domain of AP-2 and clathrin. It also binds the EH domain of Eps-15 via NPF (Asn-Pro-Phe) motifs. (*B*) TIRFM image of a COS7 cell transiently transfected with LCa-mRFP and Endo2-GFP showing spots of clathrin that colocalize with endophilin (filled arrowheads) and those that do not (open arrowheads). (*C*) Selected frames from a time series acquired every 4 s of a clathrin spot (*Top*) and endophilin (*Middle*). Merged image shows colocalization of clathrin and endophilin (*Bottom*; yellow) at a late stage in vesicle formation. (*D*) Fluorescence intensity (F.U., fluorescent units) as a function of time of a representative clathrin spot (red) and its corresponding "burst" of endophilin. (*E*) Select frames from a time series acquired every 4 s of a cell transiently transfected with Dyn2-mRFP (*Top*) and Endo2-GFP (*Middle*). Merged image (*Bottom*) shows spatial and temporal colocalization of dynamin and endophilin. (*F*) Fluorescence intensity as a function of time of the dynamin (red) and endophilin (green) spots shown in *D*. (*G*) Distribution of occurrences of endophilin appearance relative to the appearance of dynamin ($n = 99$). (*H*) Time course of fluorescence intensity of Dyn2-mRFP (red) and Endo1-GFP (green). [Scale bars: 5 (*B*), 0.5 (*C*), and 0.5 (*E*) μm.]

relationship to CCP turnover. Specifically, Endo2-GFP and clathrin-light-chain-monomeric red fluorescent protein (LCa-mRFP) were transiently coexpressed in COS7 cells and imaged by TIRFM in live cells (Fig. 1*B*). Endo2 was chosen for these experiments, because this protein is the predominant nonneuronal endophilin isoform. Transfected LCa-mRFP displayed a diffraction-limited punctate pattern characteristic of CCPs (29). Individual clathrin puncta appeared asynchronously, slowly increased in fluorescence intensity, plateaued, and then rapidly disappeared. Endo2-GFP also displayed a punctate pattern, and in double-transfected cells it colocalized as a transient burst with ≈60% of the LCa-mRFP spots (Fig. 1*B*; closed arrowheads), just before disappearance of the clathrin signal [Fig. 1 *C* and *D*; supporting information (SI) Movie 1]. The average lifetime of Endo2-GFP bursts was 27.7 ± 4 s ($n = 65$ spots from three cells). In contrast, the average CCP lifetime, as detected by LCa-mRFP, was 146.8 ± 6.5 s ($n = 112$ spots from three cells), which is consistent with other reports using TIRFM (30, 31). There was no significant difference in the lifetime of clathrin puncta positive or negative for an endophilin burst (156 ± 8 s and 133.9 ± 10.5 s, respectively; $P = 0.099$).

The timing of the endophilin burst was reminiscent of the transient recruitment of dynamin that precedes CCP disappearance. Because endophilin binds both synaptojanin and dynamin, we examined the timing of Endo2 recruitment relative to dynamin 2 (Dyn2; its nonneuronal isoform). In COS7 cells coexpressing Dyn2 tagged with mRFP (Dyn2-mRFP) and Endo2-GFP, 88% of the transient endophilin bursts colocalized with a burst of dynamin (Fig. 1*E*). Both proteins appeared and disappeared with similar kinetics (29.9 ± 1.9 s for 100 dynamin spots from three cells and 23.6 ± 1.6 s for 88 endophilin spots from three cells) (Fig. 1*F*). Furthermore, most Endo2 spots (78%) appeared together with dynamin (Fig. 1*G*). Similar observations were made upon double transfection of endophilin 1 (Endo1) and dynamin (Fig. 1*H*). We conclude that, despite the lack of clathrin-binding motifs, endophilin is recruited to CCPs where, together with dynamin, it participates in late stages of endocytosis. However, we also observed transient spots of endophilin, negative for clathrin but positive for dynamin, consistent with a role of these proteins also in clathrin-independent forms of endocytosis (data not shown).

Endophilin Mediates Recruitment of SJ1-145 to the Plasma Membrane. We next investigated the recruitment of SJ1-145 to CCPs relative to endophilin. When expressed alone in COS7 cells, GFP-SJ1-145 had a predominantly diffuse pattern (Fig. 2*A Left*), with only 17 ± 3 CCP-like puncta per cell (Fig. 2*B*); this contrasts with the highly punctate localization of fluorescently tagged clathrin, dynamin, and endophilin (compare Fig. 1 *B* and *E*). The bright signal produced by these other proteins at CCPs likely reflects their assembly into polymers or oligomers. SJ1-145, whose action is not thought to involve polymerization, may not be sufficiently concentrated at most CCPs to produce a strong signal above its diffuse cytosolic background. We speculated that if endophilin plays a role in SJ1-145 recruitment, then its overexpression may enhance SJ1-145 accumulation at endocytic spots. Indeed, when Endo1-mRFP was coexpressed with GFP-SJ1-145 in COS7 cells, 55 ± 6 GFP-SJ1-145 spots per cell were observed (Fig. 2*A Right*, arrowheads), which is >3-fold higher than in cells transfected with GFP-SJ1-145 alone (Fig. 2*B*; 8-min running average from five cells; $P = 0.0004$). Of these GFP-SJ1-145 spots, >90% colocalized with Endo1-mRFP (Fig. 2*C*). Furthermore, the fluorescence intensity of colocalized GFP-SJ1-145 and Endo1-mRFP spots synchronously increased, peaked, and decreased, suggesting a coordinated behavior (Fig. 2*D*). The average lifetimes of Endo1-mRFP and GFP-SJ1-145 spots were nearly identical (31 ± 2 s, 129 spots from four cells, and 34 ± 2 s, 119 spots from four cells, respectively) (Fig. 2*E*). Collectively, our findings are consistent with a physiological role of endophilin in the recruitment of SJ1-145 to late-stage CCPs, although they do not rule out possible roles of other proteins in such recruitment.

SJ1-170 Is Recruited to CCPs at an Early Stage. Because the C-terminal amino acid sequence unique to SJ1-170 contains binding sites for clathrin-coat components (clathrin heavy

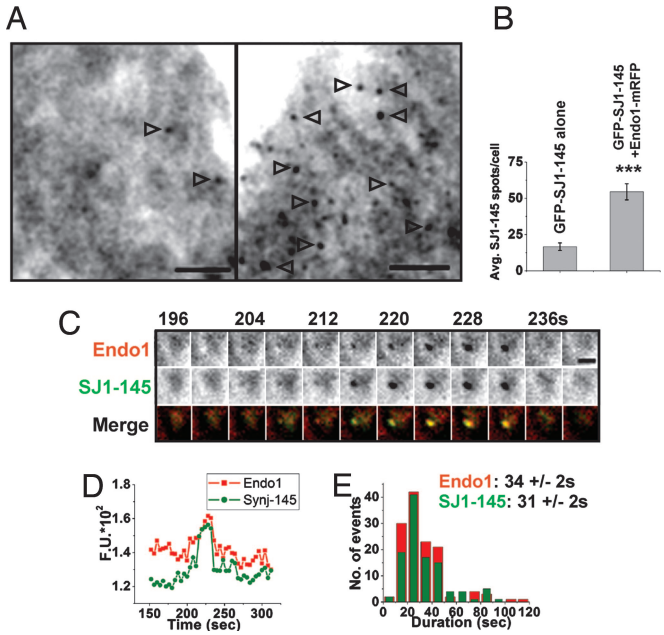

Fig. 2. Role of endophilin in the recruitment of SJ1-145 to late-stage CCPs. (*A*) GFP channel of a COS7 cell transiently transfected with GFP-SJ1-145 alone (*Left*) or GFP-SJ1-145 and mRFP-endophilin (*Right*). In the presence of exogenous endophilin (*Right*), SJ1-145 localizes to numerous punctate structures at the plasma membrane (arrowheads) as compared with cells expressing GFP-SJ1-145 alone. (*B*) Quantification of the average number of SJ1-145 spots per cell over a time interval of 8 min. (*C*) Selected frames from a time series showing colocalization of mRFP-endophilin (*Top*) and GFP-SJ1-145 (*Middle*). (*D*) Integrated fluorescence intensity as a function of time of mRFP-endophilin (red) and GFP-SJ1-145 (green) shown in *B*. (*E*) Distribution of endophilin (red) and SJ1-145 (green) lifetimes. ***, $P = 0.0004$. [Scale bars, 5 (*A*) and 0.5 (*C*) μm.]

chain, AP-2 and Eps15) (9, 12), we examined whether its recruitment differed from SJ1-145. GFP-SJ1-170 was transiently expressed in COS7 cells together with LCa-mRFP (Fig. 3*A*). In striking contrast to GFP-SJ1-145 (Fig. 2*A*), GFP-SJ1-170 had a highly punctate distribution, even when expressed alone (Fig. 3*A*). In addition, >90% of GFP-SJ1-170 colocalized in space and time with LCa-mRFP spots (Fig. 3*A*). GFP-SJ1-170 appeared approximately at the same time as LCa-mRFP (Fig. 3 *B* and *C*; SI Movie 2). Specifically, the average lifetime of LCa-mRFP spots was 119 ± 5 s (n = 120), whereas GFP-SJ1-170 spots was 113 ± 5 s (n = 113) (Fig. 3*D*). Approximately 73% of LCa-mRFP and GFP-SJ1-170 spots appeared together (Fig. 3*E*), indicating a close spatial-temporal correlation of the behavior of these two proteins. Similarly, in cells cotransfected with Dyn2-mRFP and GFP-SJ1-170 (Fig. 3*F*), a transient late-stage burst of Dyn2-mRFP was observed at ≈86% of GFP-SJ1-170 spots (Fig. 3*F*). Finally, despite the early appearance of SJ1-170, endophilin was still recruited during late stages when coexpressed (Fig. 3*G*). Together, this suggests a role for SJ1-170 not only at late stages but also during the growth phase of CCPs and demonstrates that the C-terminal extension of SJ1-170 is essential for its early recruitment to CCPs. We note that, although a potential AP-2-binding motif has been identified also in the C-terminal region of SJ1-145 (32), the absence of this protein at early-stage CCPs argues against a major role of this motif in its recruitment.

SJ1-170 Mutant Lacking 5′-Phosphatase Activity Impairs CCP Turnover. We subsequently investigated whether the PI(4,5)P_2 phosphatase activity of synaptojanin has a regulatory role on CCP dynamics. To examine this possibility, we generated a phosphatase-defective mutant of GFP-SJ1-170 and examined its effect on CCP dynamics. It was previously shown that mutation of aspartic acid 730 to alanine (D730A) within the evolutionarily conserved 5′-phosphatase module abolishes its catalytic activity (33). Whereas clathrin spots in COS7 cells cotransfected with LCa-mRFP and wild-type GFP-SJ1-170 appeared, grew, and disappeared (Figs. 3*B* and 4*A Upper*), clathrin spots present in cells cotransfected with LCa-mRFP and GFP-SJ1-170^{D730A} remained "frozen" at the cell surface (Fig. 4*A Lower*, exemplified in the color merge of three images within a 6-min interval; SI Movie 3). Quantifications from several cells revealed that 91% of clathrin spots in cells coexpressing GFP-SJ1-170^{D730A} did not turn over (were frozen) during a 10-min interval, compared with 5% in cells coexpressing wild-type GFP-SJ1-170 (Fig. 4*B*).

The effect on clathrin-coat dynamics after expression of a "5-phosphatase dead" SJ1-170 mutant was further assessed by measuring transferrin internalization, which is a clathrin-dependent process. Whereas cells expressing wild-type GFP-SJ1-170 internalized Alexa-568-labeled transferrin (Fig. 4*C Upper*), those transfected with GFP-SJ1-170^{D730A} were defective in transferrin uptake (Fig, 4*C Lower*). The strong dominant-negative effect on CCP dynamics produced by expression of the 5-phosphatase mutant SJ1-170 suggests that PI(4,5)P_2 dephosphorylation may not only be needed for clathrin uncoating after fission, but also during coat maturation.

Discussion

Here we report the spatial-temporal dynamics of endophilin and synaptojanin at CCPs. Both proteins have been implicated in clathrin-mediated endocytosis (2, 3, 9, 12, 19). However, their recruitment to CCPs in living cells remained to be demonstrated, and the timing of their recruitment had yet to be characterized. Our single CCP analysis in living cells has provided evidence for the role of these proteins in clathrin-mediated endocytosis. Furthermore, our data have yielded insight into the stage of this process at which they function and have highlighted striking differences in the dynamics of two splice variants of SJ1.

Our results support an action of SJ1-145 at a site very close to the site of dynamin action, as has been suggested (5). The similar time course of accumulation of endophilin, dynamin, and SJ1-145 at late stages in the life cycle of an endocytic pit indicates that the recruitment and function of these proteins are highly coordinated. This coordination, in turn, likely reflects a function of these proteins in closely related events, such as CCP fission and uncoating. Our results also show a very different temporal recruitment of SJ1-170, raising new questions about the role of phosphoinositide metabolism during the growth and maturation of the clathrin coat.

Endophilin lacks known binding motifs for clathrin and other coat components. Yet, as we show here in living cells, the majority of endophilin is observed at CCPs, where it is highly colocalized in space and time with dynamin. This is consistent with previous EM studies on brain membranes in cell-free systems, where endophilin localized to dynamin-coated tubular necks of CCPs (19). However, an additional localization of endophilin at necks of non-CCPs is possible, because ≈40% of endophilin spots do not colocalize with clathrin. Other structures that could recruit endophilin include caveolae (34) or micropinocytic vesicles. Although dynamin was recruited to CCPs independent of endophilin expression, the accumulation of SJ1-145 to CCPs strongly depended on the expression of endophilin, consistent with an important role of endophilin in the targeting of SJ1 (20, 21, 23).

Although we show clear evidence of endophilin recruitment during a late stage of CCP formation, exactly how it is recruited remains an open question. Potential targeting mechanisms that may function synergistically include the following: (*i*) preferen-

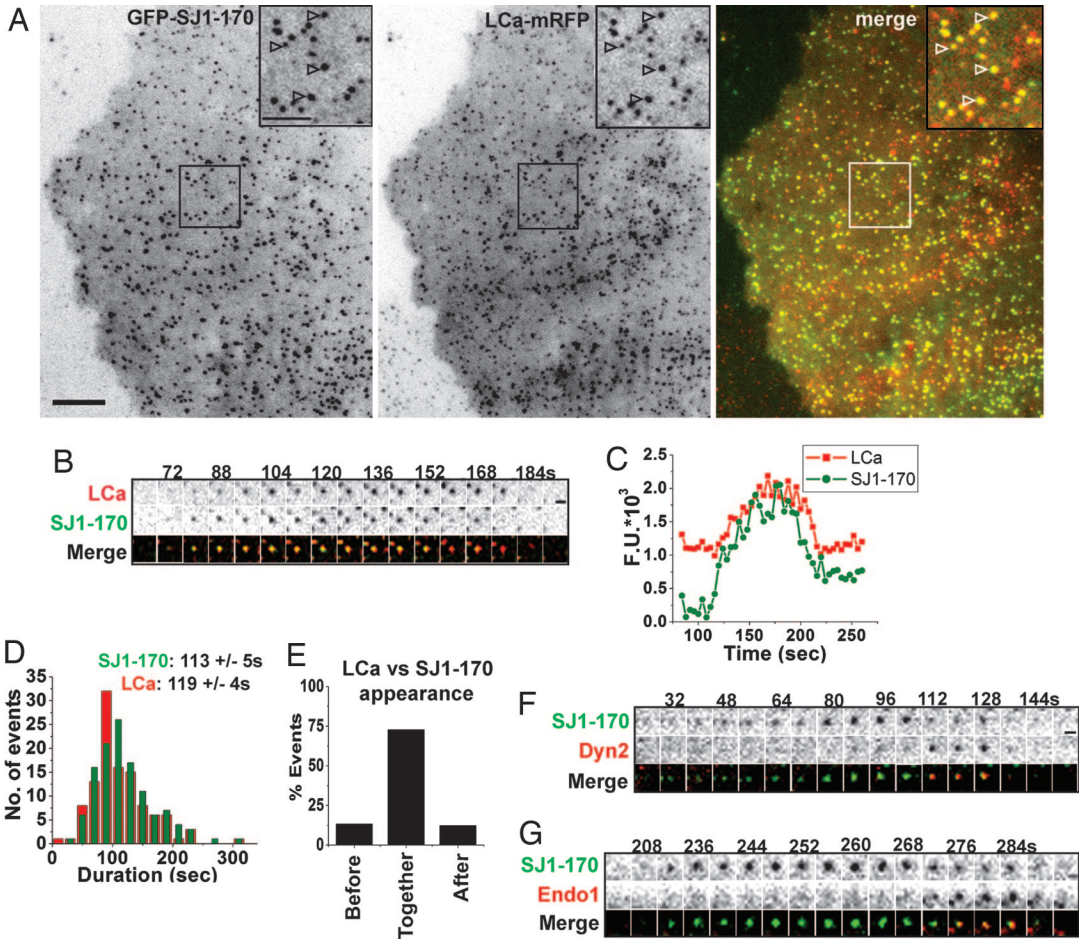

Fig. 3. SJ1-170 is recruited at an early stage during CCP formation. (*A*) COS7 cell cotransfected with GFP-SJ1-170 (green) and LCa-mRFP (red). Enlargements of *Inset* are shown at *Right*. Colocalizing spots are highlighted in the merged *Inset* (open arrowheads). (*B*) Selected frames taken from a time series of an LCa-mRFP (red) spot. GFP-SJ1-170 (green) is recruited early during the formation of a CCP and persists throughout its lifetime. (*C*) Integrated fluorescence intensity of the LCa-mRFP (red) and GFP-SJ1-170 (green shown in *C*, as a function of time). (*D*) Lifetime distribution of LCa-mRFP (red; $n = 120$) and GFP-SJ1-170 (green; $n = 113$) taken from three cells. (*E*) Distribution of occurrences of SJ1-170 appearance relative to the appearance of clathrin ($n = 112$). (*F*) Select frames taken from a time series of a GFP-SJ1-170 (green) imaged with Dyn2-mRFP (red). Dynamin is recruited and colocalizes with SJ1-170 during a late stage in CCP formation. (*G*) Selected frames from a time series acquired every 4 s of a GFP-SJ1-170 spot (*Top*) and Endo1-mRFP (*Middle*). Merged image shows colocalization of SJ1-170 and Endo1 (*Bottom*; yellow) at a late stage in vesicle formation. [Scale bars: 10 (*A*), 5 (*A Inset*), 1 (*B*), 1 (*F*), and 0.5 (*G*) μm.]

tial association by its BAR domain, with the curved membrane of the vesicle stalk (5, 18, 25, 26); (*ii*) interaction by its SH3 domain with dynamin (15); and (*iii*) binding, again by its SH3 domain, with cargo proteins present in the nascent vesicle (35–37). Because endophilin exists as a dimer (38), it may simultaneously bind two different proteins, e.g., synaptojanin and either vesicle cargo or dynamin, by the two SH3 domains of the dimer.

Recruitment of SJ1-145 may help ensure dephosphorylation of $PI(4,5)P_2$ on endocytic membranes that undergo fission (3). Consequentially, this would guarantee selective retention of $PI(4,5)P_2$ at the plasma membrane and promote uncoating of vesicles immediately after fission (5). The SJ1-mediated change in phosphoinositide composition of the newly formed endocytic vesicle may favor uncoating by decreasing the affinity of clathrin adaptors with the membrane while simultaneously promoting the recruitment of auxilin, a cofactor for the "uncoating ATPase" HSC70 (39, 40). The importance of SJ1 in clathrin uncoating is strongly supported by the accumulation of clathrin-coated vesicles in nerve terminals of SJ1 knockout mice (3, 28).

The striking colocalization of SJ1-170 with endocytic CCPs, irrespective of their maturation stage, is probably explained by the presence of interaction sites for clathrin-coat components (9, 12). However, the mere presence of binding sites for the endocytic adaptor AP-2 and the N-terminal domain of clathrin heavy chain in a protein is not sufficient to target it to a nascent CCP. This is supported, for example, by studies conducted with auxilin, which contains such domains. Indeed, auxilin, which is required for uncoating, is recruited to clathrin-coated vesicles only after fission (39–41). Our findings suggest that the phosphatase activity of SJ1-170 may play an important, although not essential (see below), role throughout the life cycle of CCPs in nonneuronal cells. Turnover of $PI(4,5)P_2$ may be needed for the normal growth of a CCP by facilitating dynamic remodeling of the coat. This possibility is consistent with a recent report that type I PIP kinases (PI4P 5-kinases), which are the major $PI(4,5)P_2$ synthesizing enzymes, interact with AP-2, even though these enzymes are apparently not concentrated at CCPs (42, 43).

Because SJ1 knockout mice have a normal prenatal development and live several hours after birth (3), the function of both SJ1-145 and SJ1-170 is clearly not essential for CCP dynamics, a housekeeping process needed in all cells. Other phosphoinositide phosphatases may have an overlapping function with SJ1 and functionally replace it in its absence. These

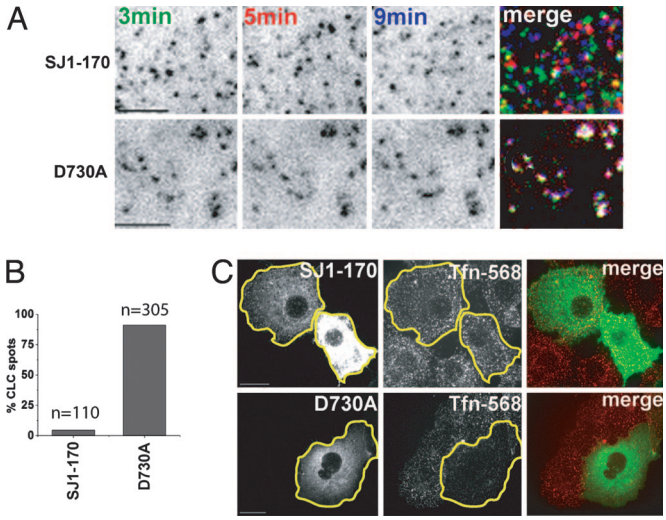

Fig. 4. A mutant SJ1-170 lacking 5′-phosphatase activity impairs CCP turnover. (*A*) Frames taken from a time series of COS7 cells transfected with GFP-SJ1-170 and LCa-mRFP (*Upper*) or GFP-SJ1-170^{D730A} and LCa-mRFP (*Lower*). Only the LCa-mRFP channel is shown. Frames corresponding to 3, 5, and 9 min were color-coded green, red, and blue, respectively, and merged. Areas showing white color reveal colocalization among all three time frames (indicating an object that did not move throughout the time series), whereas separation of the three colors indicates objects that have appeared and disappeared during the course of the image acquisition, and that do not colocalize. (*B*) Quantification of the percentage of LCa-mRFP that remains at the plasma membrane after 10 min of image acquisition in cells transfected with either GFP-SJ1-170 or GFP-SJ1-170^{D730A}. (*C*) Uptake of transferrin-Alexa 568 in COS7 cells transfected with GFP-SJ1-170 (*Upper*) or GFP-SJ1-170^{D730A} (*Lower*). Images show impaired uptake of transferrin in cells expressing GFP-SJ1-170^{D730A} (yellow outline; *Lower*) compared with GFP-SJ1-170 (yellow outline; *Upper*). [Scale bars: 5 (*A*) and 50 (*C*) μm.]

include synaptojanin 2 (44, 45) and the inositol 5-phosphatase OCRL, which, like SJ1-170, contains binding motifs for the heavy chain of clathrin as well as for AP-2 (46). The dramatic effect of a catalytically inactive SJ1-170 mutant seen here may be explained by a dominant-negative effect on the recruitment of other phosphatases. SJ1-170 is virtually absent from mature neuronal synapses, where clathrin-mediated endocytosis plays a critical role and where SJ1-145 is by far the major synaptojanin isoform (2, 13). One possibility is that SJ1-145 may be recruited early to CCPs of synapses indirectly by adaptors that bind clathrin and AP-2, such as amphiphysin, or by interactions of the endophilin dimer with synaptic vesicle cargo, such as the vesicular glutamate transporter (36, 37). Thus, the direct interaction of SJ1-170 with the clathrin coat at early stages of clathrin coat formation may be replaced, at least in part, by an indirect interaction mediated by an adaptor in nerve terminals.

In summary, our quantitative analysis of the spatial-temporal recruitment of two major endocytic proteins, endophilin and SJ1, provide insight into where and when they function during clathrin-mediated endocytosis. The unexpected finding that the nonsynaptic synaptojanin isoform, SJ1-170, is associated with CCPs throughout their life cycle raises the possibility that dynamic metabolism of PI(4,5)P_2 is essential for CCP growth and maturation at multiple stages.

Methods

Plasmids, Oligos, and Reagents. Full-length human GFP-SJ1-170 was generated by digesting pcDNA3-SJ1-170 (2) with KpnI and ApaI, isolating the SJ1-170 fragment and ligating it into peGFP-C1 (Clontech, Mountain View, CA) using KpnI and ApaI sites. GFP-SJ1-145 was generated by an identical procedure using pcDNA3-SJ1-145 (2). The D730A substitution mutation was generated by PCR with mutant primers at the D730 site and ligated into GFP-SJ1-170. Endo1 and -2-GFP were generated from pGex6p1-Endo1/2 (38) by cloning into peGFP-N1. LCa-GFP and Dyn2-GFP were gifts from James Keen (Thomas Jefferson University, Philadelphia, PA) and Mark McNiven (Mayo Clinic, Rochester, MN), respectively. Endo1, Dyn2, and LCa were subcloned into a vector encoding mRFP (kind gift of Roger Tsien, University of California at San Diego, La Jolla, CA) to produce Endo1-mRFP, Dyn2-mRFP, and LCa-mRFP. The anti-clathrin heavy chain antibody (clone TD.1) and Alexa 568-conjugated human transferrin were purchased from Sigma–Aldrich (St. Louis, MO) and Molecular Probes (Invitrogen, Carlsbad, CA), respectively.

Tissue Cell Culture, Transfection, and Reagents. COS7 cells were incubated at 37°C in 10% CO_2 in phenol red-free MEM, supplemented with 10% FBS, L-glutamine, and 100 μg/ml penicillin/streptomycin (Invitrogen). GFP- and mRFP-tagged proteins were coexpressed in COS7 cells by transfecting 1–3 μg of DNA with FuGENE 6 (Roche Diagnostics, Indianapolis, IN) or the Amaxa nucleofector kit (Amaxa, Cologne, Germany). Transfected cells were seeded in glass-bottomed 35-mm dishes (Mattek, Ashland, MA) and imaged ≈14–24 h later (50–70% confluency).

Live Cell Imaging. Before imaging, medium was replaced with an imaging buffer containing 136 mM NaCl, 2.5 mM KCl, 2 mM $CaCl_2$, 1.3 mM $MgCl_2$, and 10 mM Hepes at pH 7.4. Cells were imaged at 37°C by TIRFM using an Olympus objective-type IX-70 inverted microscope fitted with a 60× 1.45 N.A. TIRFM lens (Olympus, Melville, NY) and controlled by Andor iQ software (Andor Technologies, Belfast, Ireland). Laser lines (488 and 568 nm) from argon and argon/krypton lasers (Melles Griot, Carlsbad, CA) were coupled to the TIRFM condenser through a single optical fiber. The calculated evanescent field depth was ≈100 nm. Cells were typically imaged in two channels by sequential excitation at 0.25 Hz, without binning, with 0.2- to 0.5-s exposures and detected with a back-illuminated Andor iXon887 EMCCD camera (512 × 512, 16-bit; Andor Technologies).

Image Analysis. We used NIH Image J and Andor iQ software to analyze raw images and to generate integrated intensity plots of areas of interest, corresponding to CCP or nearby background. We calculated the lifetime of fluorescently tagged protein by manually assessing at least 80 fluorescent spots (from three different cells), which showed clear appearance (spot/background ratio >1.5) and disappearance (spot/background ratio <1.5) from the TIRFM field. Colocalization between two proteins was determined by randomly selecting 100 spots in the GFP channel, followed by manually scoring for colocalization in the RFP channel. In determining the relative time of appearance of GFP- and mRFP-tagged proteins in the same CCP, we discarded time differences of only one frame, as they could result from the sequential acquisition.

Calculation of the percentage of LCa-mRFP dots on the plasma membrane after coexpression of wild-type or SJ1-170^{D730A} was conducted by random selection of at least 100 fluorescent spots in the 5-min frame of at least three movies of 10-min duration. Spots that remained static throughout the course of the movie were scored as frozen. All data were analyzed for significance using Student's *t* test.

We thank Olympus USA for support and assistance to the Yale CINEMA laboratory. This work was supported by National Institutes of Health Grants NS36251 and CA46128, the G. Harold and Leila Y. Mathers Charitable Foundation, the Kavli Foundation, Yale/National Institute on Drug Abuse Neuroproteomic Center Grant DA018343 and Yale Diabetes and Endocrinology Research Center Grant DK45735 (to

P.D.C), the Human Frontier Science Program (Young Investigator Award RGY40/2003), Bayer Pharmaceuticals Scholar Award, the Ludwig Institute for Cancer Research (to D.T.), and a Boehringer Ingelheim Fonds PhD Scholarship (to R.Z.).

1. Giadarov I, Keen JH (1999) *J Cell Biol* 146:755–764.
2. McPherson PS, Garcia EP, Slepnev VI, David C, Zhang X, Grabs D, Sossin WS, Bauerfeind R, Nemoto Y, De Camilli P (1996) *Nature* 379:353–357.
3. Cremona O, Di Paolo G, Wenk MR, Luthi A, Kim WT, Takei K, Daniell L, Nemoto Y, Shears SB, Flavell RA, *et al.* (1999) *Cell* 99:179–188.
4. Haucke V (2005) *Biochem Soc Trans* 33:1285–1289.
5. Di Paolo G, De Camilli P (2006) *Nature* 443:651–657.
6. Brett TJ, Traub LM (2006) *Curr Opin Cell Biol* 18:395–406.
7. Guo S, Stolz LE, Lemrow SM, York JD (1999) *J Biol Chem* 274:12990–12995.
8. Woscholski R, Finan PM, Radley E, Totty NF, Sterling AE, Hsuan JJ, Waterfield MD, Parker PJ (1997) *J Biol Chem* 272:9625–9628.
9. Haffner C, Takei K, Chen H, Ringstad N, Hudson A, Butler MH, Salcini AE, Di Fiore PP, De Camilli P (1997) *FEBS Lett* 419:175–180.
10. de Heuvel E, Bell AW, Ramjaun AR, Wong K, Sossin WS, McPherson PS (1997) *J Biol Chem* 272:8710–8716.
11. Micheva KD, Kay BK, McPherson PS (1997) *J Biol Chem* 272:27239–27245.
12. Haffner C, Di Paolo G, Rosenthal JA, De Camilli P (2000) *Curr Biol* 10:471–474.
13. Ramjaun AR, McPherson PS (1996) *J Biol Chem* 271:24856–24861.
14. Micheva KD, Ramjaun AR, Kay BK, McPherson PS (1997) *FEBS Lett* 414:308–312.
15. Ringstad N, Nemoto Y, De Camilli P (1997) *Proc Natl Acad Sci USA* 94:8569–8574.
16. Cestra G, Castagnoli L, Dente L, Minenkova O, Petrelli A, Migone N, Hoffmuller U, Schneider-Mergener J, Cesareni G (1999) *J Biol Chem* 274:32001–32007.
17. Slepnev VI, De Camilli P (2000) *Nat Rev Neurosci* 1:161–172.
18. Itoh T, Erdmann KS, Roux A, Habermann B, Werner H, De Camilli P (2005) *Dev Cell* 9:791–804.
19. Ringstad N, Gad H, Low P, Di Paolo G, Brodin L, Shupliakov O, De Camilli P (1999) *Neuron* 24:143–154.
20. Gad H, Ringstad N, Low P, Kjaerulff O, Gustafsson J, Wenk M, Di Paolo G, Nemoto Y, Crun J, Ellisman MH, *et al.* (2000) *Neuron* 27:301–312.
21. Schuske KR, Richmond JE, Matthies DS, Davis WS, Runz S, Rube DA, van der Bliek AM, Jorgensen EM (2003) *Neuron* 40:749–762.
22. Verstreken P, Kjaerulff O, Lloyd TE, Atkinson R, Zhou Y, Meinertzhagen IA, Bellen HJ (2002) *Cell* 109:101–112.
23. Verstreken P, Koh TW, Schulze KL, Zhai RG, Hiesinger PR, Zhou Y, Mehta SQ, Cao Y, Roos J, Bellen HJ (2003) *Neuron* 40:733–748.
24. Dickman DK, Lu Z, Meinertzhagen IA, Schwarz TL (2006) *Curr Biol* 16:591–598.
25. Farsad K, Ringstad N, Takei K, Floyd SR, Rose K, De Camilli P (2001) *J Cell Biol* 155:193–200.
26. Peter BJ, Kent HM, Mills IG, Vallis Y, Butler PJ, Evans PR, McMahon HT (2004) *Science* 303:495–499.
27. Itoh T, De Camilli P (2006) *Biochim Biophys Acta* 1761:897–912.
28. Kim WT, Chang S, Daniell L, Cremona O, Di Paolo G, De Camilli P (2002) *Proc Natl Acad Sci USA* 99:17143–17148.
29. Gaidarov I, Santini F, Warren RA, Keen JH (1999) *Nat Cell Biol* 1:1–7.
30. Merrifield CJ, Feldman ME, Wan L, Almers W (2002) *Nat Cell Biol* 4:691–698.
31. Merrifield CJ, Perrais D, Zenisek D (2005) *Cell* 121:593–606.
32. Praefcke GJ, Ford MG, Schmid EM, Olesen LE, Gallop JL, Peak-Chew SY, Vallis Y, Babu MM, Mills IG, McMahon HT (2004) *EMBO J* 23:4371–4383.
33. Jefferson AB, Majerus PW (1996) *Biochemistry* 35:7890–7894.
34. Yao Q, Chen J, Cao H, Orth JD, McCaffery JM, Stan RV, McNiven MA (2005) *J Mol Biol* 348:491–501.
35. Tang Y, Hu LA, Miller WE, Ringstad N, Hall RA, Pitcher JA, DeCamilli P, Lefkowitz RJ (1999) *Proc Natl Acad Sci USA* 96:12559–12564.
36. Vinatier J, Herzog E, Plamont MA, Wojcik SM, Schmidt A, Brose N, Daviet L, El Mestikawy S, Giros B (2006) *J Neurochem* 97:1111–1125.
37. Voglmaier SM, Kam K, Yang H, Fortin DL, Hua Z, Nicoll RA, Edwards RH (2006) *Neuron* 51:71–84.
38. Ringstad N, Nemoto Y, De Camilli P (2001) *J Biol Chem* 276:40424–40430.
39. Massol RH, Boll W, Griffin AM, Kirchhausen T (2006) *Proc Natl Acad Sci USA* 103:10265–10270.
40. Lee DW, Wu X, Eisenberg E, Greene LE (2006) *J Cell Sci* 119:3502–3512.
41. Sever S, Skoch J, Newmyer S, Ramachandran R, Ko D, McKee M, Bouley R, Ausiello D, Hyman BT, Bacskai BJ (2006) *EMBO J* 25:4163–4174.
42. Loijens JC, Anderson RA (1996) *J Biol Chem* 271:32937–32943.
43. Krauss M, Kukhtina V, Pechstein A, Haucke V (2006) *Proc Natl Acad Sci USA* 103:11934–11939.
44. Nemoto Y, Wenk MR, Watanabe M, Daniell L, Murakami T, Ringstad N, Yamada H, Takei K, De Camilli P (2001) *J Biol Chem* 276:41133–41142.
45. Rusk N, Le PU, Mariggio S, Guay G, Lurisci C, Nabi IR, Corda D, Symons M (2003) *Curr Biol* 13:659–663.
46. Lowe M (2005) *Traffic* 6:711–719.